ORIGINAL PAPER

Development of biopolymer electrolyte membrane using Gellan gum biopolymer incorporated with NH$_4$SCN for electro-chemical application

R. Meera Naachiyar [1,2] · M. Ragam [1] · S. Selvasekarapandian [2,3] · M. Vengadesh Krishna [2] · P. Buvaneshwari [2,4]

Abstract

Based on the biopolymer Gellan gum with ammonium thiocyanate (NH$_4$SCN) salt, solid electrolyte has been prepared with distilled water as solvent, using solution casting technique. The prepared solid electrolytes are subjected to various characterization techniques such as XRD, FTIR, DSC, and Ac impedance technique. Amorphous/crystalline nature of biopolymer membrane is studied by XRD. The polymer–salt complex formation has been studied by FTIR technique. Biopolymer membrane of 1 g Gellan gum with 1.1 M wt% of NH$_4$SCN exhibits very high amorphous nature with a high proton conductivity of 1.41×10^{-2} S/cm and a glass transition temperature (T_g) of 42.98 °C. Using the highest ionic conducting biopolymer electrolyte, proton battery and fuel cell have been fabricated and their performance is studied. Proton battery constructed shows the open circuit voltage of *1.62 V*. A single fuel cell constructed using the highest conducting membrane gives the voltage of *580 mV*.

Keywords Biopolymer · Gellan gum · Ac impedance study · Proton battery · Fuel cell

Introduction

The human life is unpleasant without the use of electronic devices. The life span of the electronic device depends on its power sources such as battery and components of battery. The performance of the battery depends on its electrolyte. This electrolyte must fulfill the following requirements such as safety, consistent performance/accuracy, and stability there by making the process easier for the ion transportation [1, 2]. The electrolytes are of various types like liquid electrolyte, solid electrolyte, and polymer electrolyte. In the realm of polymer electrolyte, the proton conducting polymer electrolyte has received considerable attention in the view of their perspective applications in electrochemical devices such as solid state

batteries, fuel cells, dye sensitized solar cell, super capacitors, humidity sensor, gas sensors, and electrochemical windows [3–13].

The main preference towards the solid polymer electrolyte in solid state ionic devices raises due to their film forming capacity of different size, flexibility, mechanical strength, processability, ability of ion transportation, electrochemical stability, proper electrode–electrolyte contact, safety, long life, no leakage, and light weight [14–16]. Blending of two polymers, adding of inorganic filters, use of grafts, block co-polymer, and adding plasticizers to the polymers are the methods that can improve the properties of electrolytes [14–18].

Various types of solid polymer electrolytes such as PVC [19], PAN [20–24], PVP [25], PEO [26], PVA [27–31], PGS [32], and PMMA [33] have been explored in the development of solid electrolyte system. But these polymers are synthetic-based polymers. They posses very high cost and are non-biodegradable. The renewable form of energy is essential in recent days to overcome the challenges like power crisis and environmental pollution. Keeping the caution of environment pollution and the cost efficiency in mind, the researchers recently work on the development of natural polymers as electrolyte, which will be a promising substitute to the synthetic polymers. The preference towards the natural polymers is due

✉ S. Selvasekarapandian
   sekarapandian@rediffmail.com

1   Fatima College, Madurai, Tamil Nadu 625018, India

2   Materials Research Center, Coimbatore, Tamil Nadu 641045, India

3   Bharathiar University, Coimbatore, Tamil Nadu 641046, India

4   N.M.S.S.V.N. College, Nagamalai, Madurai, Tamil Nadu 625019, India

to their abundant, environment friendly and biodegradable nature, and very good mechanical and electrical properties. Among the natural polymers, polysaccharides have good potential as hosts for ionic conduction since they are cheap and eco-friendly. The polysaccharides such as cellulose acetate, starch, pectin, carbonyl methyl cellulose, carrageenan, tamarind seed, chitosan, agar-agar, and gums are used as polymer electrolytes in the electrochemical devices [34–46]. S. Selvalakshmi et al. has reported that the composition of 50 agar: 50 NH$_4$SCN gives the conductivity of about 1.03×10^{-3} S/cm [36]. S. Monisha et al. reported the conductivity of 1.02×10^{-3} S/cm for the sample 50CA:50NH$_4$NO$_3$ [38]. M. Premalatha et al. has reported the conductivity of 1.58×10^{-3} S/cm for the composition, 1 g TSP:0.4 g NH$_4$Br [40]. G. Nirmala devi et al. has reported for the composition, 60Dextrin:40NH$_4$SCN providing the conductivity of 4.05×10^{-4} S/cm [41]. M. Muthukrishanan et al. reported for the bio polymer composition 40 Pectin: 60 NH$_4$SCN having the conductivity, 1.5×10^{-3} S/cm [42]. S. Karthikeyan et al. has reported that 80% I-carrageenan: 20 wt% NH$_4$Br gives the highest conductivity 1.08×10^{-3} S/cm [44], etc.

In the present work, the Gellan gum polymer is taken as the host polymer. Gellan gum is a water-soluble anionic polysaccharide, produced by the bacterium, *Sphingomonous Elodea* [47, 48]. It is a multifunctional gelling agent. It can be used alone or can be used with other products to obtain a wide interesting character, including the thermo-reversible membranes (that shows the reversible properties under heating and cooling). From the view of chemical structure, the Gellan gum is a heteropolysaccharide composed of complex tetrasaccharide repeating unit consisting of α-L-rhamnose (Rha), β-D-glucose (Glc), and β-D-glucoronic acid (GlcA) in the ratio of 1:2:1. Figure 1 shows the structure of Gellan gum. It has been chosen because it contains good amount of –OH group, to which cation of any salt can be attached to increase the charge carrier. These are available as low acyl that forms hard, brittle gels and high acyl that forms soft, elastic, not brittle gels. This means that they can produce gel texture ranging from hard and brittle to fluid.

For the development of new contact lenses in the field of ophthalmology, the Gellan gum is very helpful. As the Gellan gum is edible, they are used in the food industry as a stabilizer and food thickener [49–51].

The unique property of Gellan gum is its ability of producing solutions with low viscosity [49, 51]. Another important property is that it has high thermal stability up to 120 °C and highly transparent, because of which they can be applied in electrochemical devices too. Due to abundance availability, low cost, and easier process ability, the Gellan gum can also be a best replacer in the biopolymer line for the non bio-degradable, toxic, and harmful materials used in the commercial electrochemical devices. Literature survey reveals that there are very few reports in Gellan gum. S.R. Majid et al. has studied lithium ion conductivity in Gellan gum blended with PVP using LiClO$_4$ [52]. I.S.M. Noor reported study of Gellan gum with LiCF$_3$SO$_4$ [53, 54].

Ammonium salts are reported as they are very good proton donors to the polymer matrix. The protonic transport in the polymer membrane generally involves the motion of H+ ion. Preparation of biopolymers with the ammonium salts has attracted many researchers for the development of high conducting biopolymer electrolyte. [29–32, 34–46, 55–57].

The objective of the present work is to synthesize the electrolyte with a higher conductivity value and to apply the polymer film for the electrochemical devices. The polymer electrolyte based on Gellan gum doped with NH$_4$SCN was prepared, and the characterization was done using XRD for its amorphous nature, FTIR for its chemical bonding, DSC for the determination of glass transition temperature, and Ac impedance spectroscopy for its conductivity measurement. Proton battery and fuel cell have been fabricated, and their performance are studied.

Experimental method

Materials and preparation

For the synthesis of the biopolymer electrolyte, the simplest technique known as Solution Casting Technique has been employed. In this work, the polymer, Gellan gum (Sisco Research Laboratories Pvt. Ltd, India), is used as the raw material. Double distilled pure water is used as the solvent to dissolve the polymer. As the gelling temperature of the Gellan gum is 35–40 °C (2% soln), to maintain the aqueous form and to dissolve, the distilled water is heated above 90 °C and 1 g Gellan gum was added pinch by pinch and stirred thoroughly

Fig. 1 Structure of Gellan gum
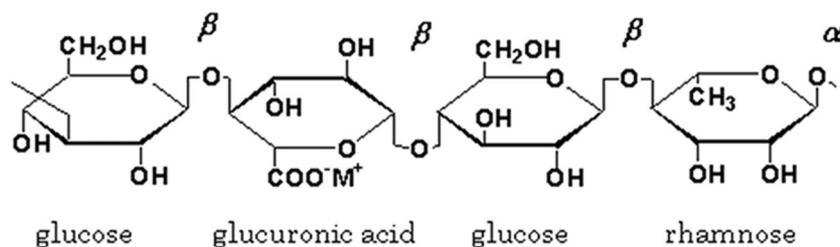
using the magnetic stirrer. And then, the various M wt % (0.8 M wt%, 1.0 M wt%, 1.1 M wt%, 1.2 M wt%) of Ammonium Thiocyanate (Merck Specialities Private Limited, India) were added to the host polymer. The solution of various compositions were casted in the petri dishes and kept in the hot air oven for around 60–80 °C for evaporation. After 12 h, fine transparent free standing films of approximately 0.2- to 0.3-mm thickness were obtained. The obtained films were subjected for various technical characterizations.

Characterization techniques

XRD

Using XRD, amorphous/crystalline nature of membrane was studied. The XRD diffraction patterns for the samples were obtained using the X'Pert PRO diffractometer using Cu-Kα radiation operated with 40 kV/30 mA in the angle range (2θ) of 10–80° at the rate of 2°/min.

FTIR

FTIR is meant for the vibrational study of the polymer membrane. The prepared polymer membranes are subjected in the SHIMADZU–IR Affinity-1 Spectrometer for the FTIR spectra record. The spectra were recorded in transmission mode in the range of 500–4000 cm^{-1} at room temperature with the resolution of 1 cm^{-1}. FTIR spectroscopy is performed by direct acquisition method.

Impedance study

The Ac impedance measurement studies for the prepared samples were carried out by the HIOKI-3532 LCR HiTester in the frequency range of 42 Hz to 5 MHz.

Thermal studies

The thermal studies were done by the DSC measurement. The DSC measurements were performed using the DSC Q20 V24.11 Build 124 under nitrogen atmosphere in the temperature range from 20 to 200 °C at the heating rate of 10 °C/min.

Electrochemical discharge studies

Solid state battery is fabricated with the configuration, Zn + $ZnSO_4$. $7H_2O$ + C‖1 g Gellan Gum + 1.1 M wt % of NH$_4$SCN‖PbO_2 + V_2O_5 + C + electrolyte, and the discharge characteristics were studied at the ambient temperature.

Transference number measurement

The transference number measurement is done using the Wagner's Polarization Technique with stainless steel electrodes to find the dominant transport member.

Results and discussions

XRD

X-ray diffraction (XRD) analysis deals with the study of crystalline/amorphous nature of the synthesized biopolymer electrolyte. Figure 2 represents the XRD peaks of Pure 1 g Gellan gum and 1 g Gellan gum with various compositions such as 0.8 M wt% of NH_4SCN, 1.0 M wt% of NH_4SCN, 1.1 M wt% of NH_4SCN, and 1.2 M wt% of NH_4SCN salts.

The Pure Gellan gum shows intense peak at an angle of 2θ = 6°, 10°, 19°, and 22°, which agrees with earlier report [51]. The XRD pattern of 1 g pure Gellan gum with different concentrations of NH_4SCN salt (0.8, 1.0, 1.1, and 1.2 M wt%) exhibits peaks at 2θ = 6°, 10°, 17°, 19°, and 22° (Fig. 3). The peaks at 6° and 10° decrease in intensity for the 0.8, 1.0, and 1.1 M wt% of NH_4SCN salt with Gellan gum. For the 1.2 M wt% of NH_4SCN salt with Gellan gum, the intensity of the peaks at 6° and 10° slightly increase. Intensity of the peaks at 17°, 19°, and 22° decreases as the concentration of the salt

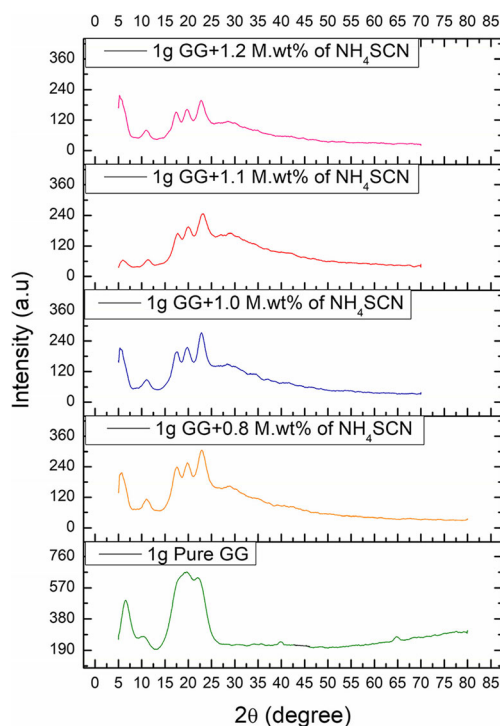Fig. 2 XRD pattern of 1 g pure Gellan gum and various compositions namely 1 g Gellan Gum: 0.8 M wt% of NH_4SCN, 1 g Gellan gum: 1.0 M wt% of NH_4SCN, 1 g Gellan gum: 1.1 M wt% of NH_4SCN, and 1 g Gellan Gum: 1.2 M wt% of NH_4SCN
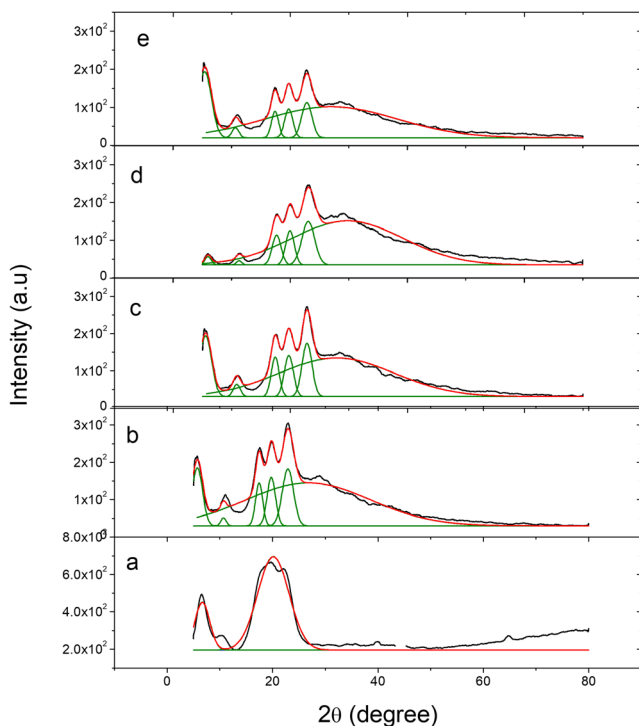
Fig. 3 Deconvoluted XRD pattern of **a** 1 g pure Gellan gum, **b** deconvoluted XRD pattern of 1 g Gellan gum: 0.8 M wt% of NH$_4$SCN, **c** deconvoluted XRD pattern of 1 g Gellan gum: 1.0 M wt% of NH$_4$SCN, **d** deconvoluted XRD pattern of 1 g Gellan gum: 1.1 M wt% of NH$_4$SCN, and **e** deconvoluted XRD pattern of 1 g Gellan gum: 1.2 M wt% of NH$_4$SCN

Table 1 Percentage of crystallinity calculated from deconvoluted XRD graph

Compositions	% of crystallinity
1 g pure Gellan gum	33.76%
1 g Gellan gum + 0.8 M wt% of NH$_4$SCN	22.65%
1 g Gellan gum + 1.0 M wt% of NH$_4$SCN	11.75%
1 g Gellan gum + 1.1 M wt% of NH$_4$SCN	*8.85%*
1 g Gellan gum + 1.2 M wt% of NH$_4$SCN	11.57%

Italic emphasizes low crystallinity percentage

doped Gellan gum, it is found that there is a decrease in crystallinity % for increase in M wt% of the salt. For the polymer electrolyte composition, 1 g Gellan gum with 1.1 M wt% of NH$_4$SCN, the crystallinity is comparatively very less, indicating more amorphous nature. Further for the highest concentration, 1 g Gellan gum with 1.2 M wt% of NH$_4$SCN, the crystallinity increased.

FTIR

Fourier transform infrared (FTIR) spectroscopy is a versatile technique used to study the complex formation between the host polymer and the salt. The FTIR spectra of pure Gellan gum and Gellan gum with various concentrations of salt (0.8, 1.0, 1.1, 1.2 M wt% of NH$_4$SCN) were represented in the Figs. 4 a and b below.

Assignments of observed peaks are provided in Table 2. About 1040 cm^{-1} peak assigned to C–O stretching [39, 54, 59] for pure Gellan gum has been found at 1039 cm^{-1}, 1036 cm^{-1}, 1033 cm^{-1}, and 1030 cm^{-1} for 1 g Gellan gum: 0.8 M wt% of NH$_4$SCN, 1 g Gellan gum: 1.0 M wt% of NH$_4$SCN, 1 g Gellan gum: 1.1 M wt% of NH$_4$SCN, and 1 g Gellan gum: 1.2 M wt% of NH$_4$SCN, respectively.

About 1066 cm^{-1} peak observed for pure Gellan gum is ascribed to CH$_2$–OH stretching [30, 54]. This peak (1066 cm^{-1}) has been shifted to 1070 cm^{-1}, 1072 cm^{-1}, 1073 cm^{-1}, and 1074 cm^{-1} for 1 g Gellan gum: 0.8 M wt% of NH$_4$SCN, 1 g Gellan gum: 1.0 M wt% of NH$_4$SCN, 1 g Gellan gum: 1.1 M wt% of NH$_4$SCN, and 1 g Gellan gum: 1.2 M wt% of NH$_4$SCN, respectively.

The peaks 1307 cm^{-1}, 1306 cm^{-1}, 1305 cm^{-1}, and 1304 cm^{-1} observed in 1 g Gellan gum: 0.8 M wt% of NH$_4$SCN, 1 g Gellan gum: 1.0 M wt% of NH$_4$SCN, 1 g Gellan gum: 1.1 M wt% of NH$_4$SCN, and 1 g Gellan gum: 1.2 M wt% of NH$_4$SCN, respectively, are attributed to C-N stretching [24, 59].

Peak observed at 1421 cm^{-1} assigned to C–C stretching [41, 42, 53, 60] for pure Gellan gum has been shifted to 1425 cm^{-1}, 1423 cm^{-1}, 1422 cm^{-1}, and 1420 cm^{-1} for 1 g Gellan gum: 0.8 M wt% of NH$_4$SCN, 1 g Gellan gum: 1.0 M

increases (0.8, 1.0, and 1.1 M wt% with NH$_4$SCN salts with Gellan gum). For biopolymer electrolyte 1 g Gellan gum with 1.2 M wt% of NH$_4$SCN, the intensity of peaks at 17°, 19°, and 22° increases.

It is observed that broadness of biopolymer electrolyte 1 g Gellan gum with different concentration of NH$_4$SCN increases compared to pure Gellan gum. The broadness is maximum for biopolymer electrolyte 1 g Gellan gum with 1.1 M wt% of NH$_4$SCN. Results of intensity and broadness of membranes are in agreement with criteria suggested by Hodge et al [58]. Peaks due to NH$_4$SCN are not found in the biopolymer electrolyte Gellan gum with different concentration of NH$_4$SCN. This indicates complete dissociation of salt.

The percentage of crystallinity has been calculated from the formula using the deconvoluted XRD graph (xure 3)

Percentage of Crystallinity (%C)

$$= \frac{\text{Area under crystalline region}}{\text{Total area of the peak}} \times 100\%$$

The crystallinity percentage of the Pure Gellan gum is found to be higher compared to the salt doped compositions of Gellan gum, represented in Table 1. On analyzing the crystallinity % for the various concentrations of NH$_4$SCN salt-
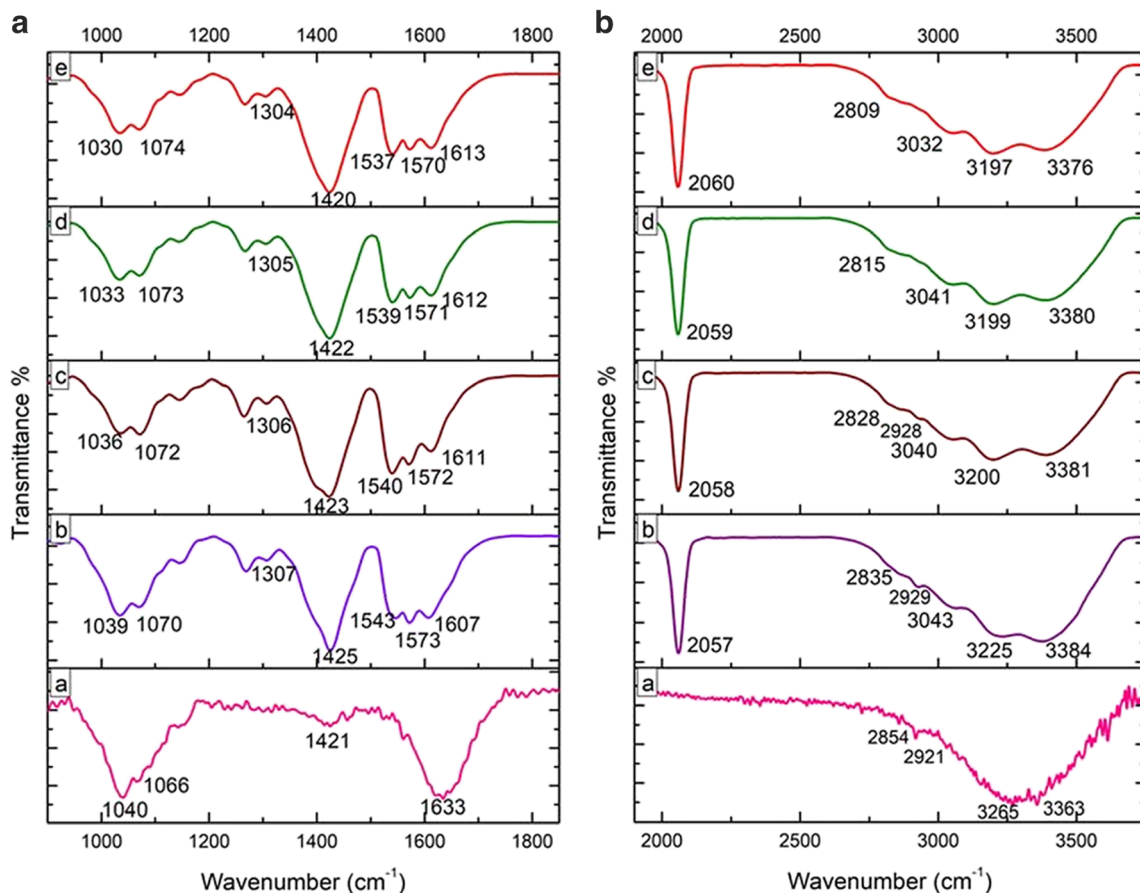
Fig. 4 a FTIR spectra of (a) pure Gellan gum, (b) 1 g Gellan gum: 0.8 M wt% of NH$_4$SCN, (c) 1 g Gellan gum: 1.0 M wt% of NH$_4$SCN, (d) 1 g Gellan gum: 1.1 M wt% of NH$_4$SCN, and (e) 1 g Gellan gum: 1.2 M wt% of NH$_4$SCN from wavenumber 400 to 1850 cm^{-1} **b** FTIR spectra of (a) pure Gellan gum (b), 1 g Gellan gum: 0.8 M wt% of NH$_4$SCN, (c) 1 g Gellan gum: 1.0 M wt% of NH$_4$SCN, (d) 1 g Gellan gum: 1.1 M wt% of NH$_4$SCN, and (e) 1 g Gellan gum: 1.2 M wt% of NH$_4$SCN from wavenumber 1850 to 4000 cm^{-1}

Table 2 FTIR assignments for Pure Gellan gum and Gellan gum with different compositions of NH$_4$SCN

Pure Gellan gum	Vibrational peaks of 1 g Gellan gum: X M wt % of NH$_4$SCN (cm^{-1})				Attributions	Reference
	X = 0.8	X = 1.0	X = 1.1	X = 1.2		
1040	1039	1036	1033	1030	C–O stretching	[39, 54, 59]
1066	1070	1072	1073	1074	CH$_2$–OH stretching	[30, 54]
-	1307	1306	1305	1304	C–N stretching	[24, 59]
1421	1425	1423	1422	1420	C–C stretching	[41, 42, 53, 60]
-	1543	1540	1539	1537	NH$_3^+$	[30]
-	1573	1572	1571	1570	NH$_3^+$	[30]
1633	1607	1611	1612	1613	(Glycosidic bond) C=O stretching	[53, 61, 62]
-	2057	2058	2059	2060	S=C=N stretching	[45]
2854	2835	2828	2615	2809	CH$_2$ Symmetric stretching	[63]
2921	2929	2928	-	-	CH$_2$ asymmetric stretching	[62, 63]
-	3043	3040	3041	3032	NH$_3^+$	[30]
3265	3225	3200	3199	3197	N–H stretching	[59]
3363	3384	3381	3380	3376	O–H stretching	[53, 59, 60, 62]

wt% of NH_4SCN, 1 g Gellan gum: 1.1 M wt% of NH_4SCN, and 1 g Gellan gum: 1.2 M wt% of NH_4SCN, respectively.

The peaks 1543 cm^{-1}, 1540 cm^{-1}, 1539 cm^{-1}, and 1537 cm^{-1} observed for 1 g Gellan gum: 0.8 M wt% of NH_4SCN, 1 g Gellan gum: 1.0 M wt% of NH_4SCN, 1 g Gellan gum: 1.1 M wt% of NH_4SCN, and 1 g Gellan gum: 1.2 M wt% of NH_4SCN, respectively, are assigned to NH_3^+ vibration [30]. Also, the peaks 1573 cm^{-1}, 1572 cm^{-1}, 1571 cm^{-1}, and 1570 cm^{-1} observed for 1 g Gellan gum: 0.8 M wt% of NH_4SCN, 1 g Gellan gum: 1.0 M wt% of NH_4SCN, 1 g Gellan gum: 1.1 M wt% of NH_4SCN, and 1 g Gellan gum: 1.2 M wt% of NH_4SCN, respectively, are assigned to NH_3^+ vibration [30]. The peaks observed for NH_3^+ vibration are not found in pure Gellan gum. This confirms the complex formation between polymer and NH_4SCN.

Peak observed at 1633 cm^{-1} attributed to C=O stretching (which is Glycosidic bond) [53, 61, 62] for pure Gellan gum has been shifted to 1607 cm^{-1}, 1611 cm^{-1}, 1612 cm^{-1}, and 1613 cm^{-1} for 1 g Gellan gum: 0.8 M wt% of NH_4SCN, 1 g Gellan gum: 1.0 M wt% of NH_4SCN, 1 g Gellan gum: 1.1 M wt% of NH_4SCN, and 1 g Gellan gum: 1.2 M wt% of NH_4SCN, respectively.

Peaks at 2057 cm^{-1}, 2058 cm^{-1}, 2059 cm^{-1}, and 2060 cm^{-1} for 1 g Gellan gum: 0.8 M wt% of NH_4SCN, 1 g Gellan gum: 1.0 M wt% of NH_4SCN, 1 g Gellan gum: 1.1 M wt% of NH_4SCN, and 1 g Gellan gum: 1.2 M wt% of NH_4SCN, respectively, which is absent in pure Gellan gum, is attributed to S=C=N stretching [45]. This indicates the complexation of NH_4SCN with polymer matrix.

The peak observed at 2854 cm^{-1} in pure Gellan gum is shifted to 2835 cm^{-1}, 2828 cm^{-1}, 2615 cm^{-1}, and 2809 cm^{-1} for 1 g Gellan gum: 0.8 M wt% of NH_4SCN, 1 g Gellan gum: 1.0 M wt% of NH_4SCN, 1 g Gellan gum: 1.1 M wt% of NH_4SCN, and 1 g Gellan gum: 1.2 M wt% of NH_4SCN attributed to CH_2 symmetric stretching [63].

The peak observed at 2921 cm^{-1} in pure Gellan gum is shifted to 2929 cm^{-1} and 2928 cm^{-1} for 1 g Gellan gum: 0.8 M wt% of NH_4SCN and 1 g Gellan gum: 1.0 M wt% of NH_4SCN are attributed to CH_2 asymmetric stretching [62, 63]. And these peaks are not found in 1 g Gellan gum: 1.1 M wt% of NH_4SCN and 1 g Gellan gum: 1.2 M wt% of NH_4SCN.

Peaks 3043 cm^{-1}, 3040 cm^{-1}, 3041 cm^{-1}, and 3032 cm^{-1} observed in 1 g Gellan gum: 0.8 M wt% of NH_4SCN, 1 g Gellan gum: 1.0 M wt% of NH_4SCN, 1 g Gellan gum: 1.1 M wt% of NH_4SCN, and 1 g Gellan gum: 1.2 M wt% of NH_4SCN, respectively, are assigned to NH_3^+ vibration [30].

The peak observed in pure Gellan gum, 3265 cm^{-1}, is shifted to 3225 cm^{-1}, 3200 cm^{-1}, 3199 cm^{-1}, and 3197 cm^{-1} observed in 1 g Gellan gum: 0.8 M wt% of NH_4SCN, 1 g Gellan gum: 1.0 M wt% of NH_4SCN, 1 g Gellan gum: 1.1 M wt% of NH_4SCN, and 1 g Gellan gum: 1.2 M wt% of NH_4SCN, respectively, are attributed to N–H stretching vibration [59]. This confirms the complex formation between the Gellan gum polymer and NH_4SCN salt.

The peak 3363 cm^{-1} assigned to O–H stretching [53, 59, 60, 62] for pure Gellan gum has been shifted to 3384 cm^{-1}, 3381 cm^{-1}, 3380 cm^{-1}, and 3376 cm^{-1} for 1 g Gellan gum: 0.8 M wt% of NH_4SCN, 1 g Gellan gum: 1.0 M wt% of NH_4SCN, 1 g Gellan gum: 1.1 M wt% of NH_4SCN, and 1 g Gellan gum: 1.2 M wt% of NH_4SCN respectively.

The shift in frequencies, change in peak intensity, and the appearance of the new peaks are due to the interaction between the salt and the polymer matrices which confirm the complex formation between the salt NH_4SCN and the biopolymer Gellan gum. The possible interaction of the NH_4SCN salt with Gellan gum is represented in Fig. 5.

Thermal analysis

Differential scanning calorimetry (DSC) is used to calculate the glass transition temperature of prepared polymer electrolyte. The DSC thermogram of pure Gellan gum and 1 g Gellan gum with different concentrations of salt (0.8 M wt% of NH_4SCN, 1.0 M wt% of NH_4SCN, 1.1 M wt% of NH_4SCN, and 1.2 M wt% of NH_4SCN) are shown in Fig. 6.

The T_g value of pure Gellan gum is 43.98 °C. On addition of NH_4SCN salt with 1 g pure Gellan gum, the T_g value increases. This increase in T_g value of 45.15 °C and 72.96 °C for the addition of 0.8 M wt% and 1.0 Mwt % of NH_4SCN salt with Gellan gum is due to the strong transient cross-linkage between oxygen atom and proton. This interaction leads to increase of microviscosity and stiffness in the polymer chain [39]. Further, for the concentration 1.1 M wt% of NH_4SCN salt with Gellan gum, the T_g value is found to be decreased. This is because of reduction of transient cross-linkage between oxygen atom and proton. This leads to the softening of the polymer [39]. For the highest concentration 1.2 M wt% of NH_4SCN salt with Gellan gum, the T_g value is increased. The glass transition temperature for pure Gellan gum and various compositions of NH_4SCN with Gellan gum are provided in Table 3. Similar form of DSC results is observed in TSP biopolymer with NH_4SCN [39].
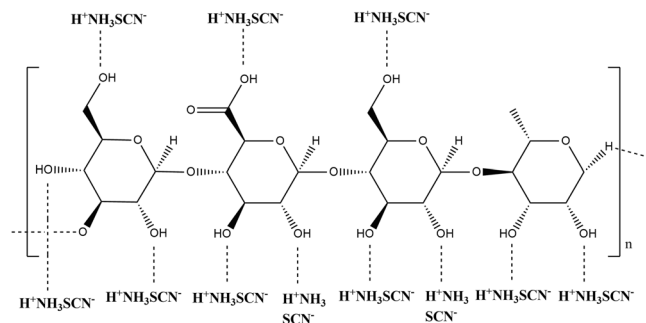

Fig. 5 Possible interaction of NH_4SCN salt with Gellan gum polymer
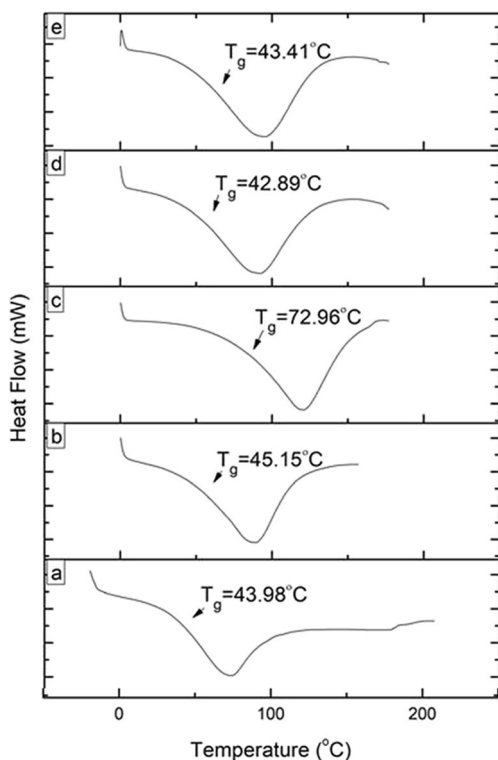
Fig. 6 DSC thermograms of **a** pure Gellan gum, **b** 1 g Gellan gum: 0.8 M wt% of NH$_4$SCN, **c** 1 g Gellan gum: 1.0 M wt% of NH$_4$SCN, **d** 1 g Gellan gum: 1.1 M wt% of NH$_4$SCN, and **e** 1 g Gellan gum: 1.2 M wt% of NH$_4$SCN

Ac impedance spectroscopy

The cole-cole plot is drawn between the real part of the impedance (Z′) and the imaginary part of the impedance (Z″) of any material, which gives the combination of high-frequency semicircle followed by the low-frequency straight line [64].

High-frequency semicircle is due to the parallel combination of bulk resistance and bulk capacitance. The resistor owes to the migration of ions that occur through the free volume of polymer matrix and the capacitor owes to the polarization of immobile (static) polymer chains in the alternating field. The low-frequency straight line is due to the electrode-electrolyte interface [64].

Table 3 Glass transition temperature for Pure Gellan gum and various compositions of NH$_4$SCN with Gellan gum

Compositions	(T$_g$)
1 g pure Gellan gum	43.98 °C
1 g Gellan gum + 0.8 M wt% of NH$_4$SCN	45.15 °C
1 g Gellan gum + 1.0 M wt% of NH$_4$SCN	72.96 °C
1 g Gellan gum + 1.1 M wt% of NH$_4$SCN	*42.98 °C*
1 g Gellan gum + 1.2 M wt% of NH$_4$SCN	43.41 °C

Italic emphasizes low T$_g$ value

In the present work, for pure system, pure Gellan gum polymer, Cole-cole plot shows a semicircle with a spike. On adding various composition of (0.8, 1.0, 1.1, 1.2 M wt %) NH$_4$SCN salt, the cole-cole plot shows only inclined straight line. Figures 7a and 8b represent the cole-cole plot of Gellan gum and the various compositions of NH$_4$SCN salt with Gellan gum. The bulk resistance (R$_b$) of the electrolyte was calculated using the Boukamp's EQ Software [65]. The EIS parameters for all the polymer electrolytes are tabulated in Table 4. The equivalent electrical circuits are shown in Figs. 7b and 8b.

From Table 4 we could infer that the bulk resistance, R$_b$, decreases with increase in salt concentrations with the bio-polymer Gellan gum. The R$_b$ value for Pure Gellan gum is 1646 Ω. The R$_b$ values for 1 g Gellan gum with various compositions of (0.8, 1.0, 1.1, 1.2 M wt %) NH$_4$SCN salt are 729 Ω, 94 Ω, 49 Ω, and 64 Ω, respectively. The impedance of constant phase element (CPE) is represented as

$$Z_{CPE} = \frac{1}{Q_0(j\omega)^n}$$

where Q_0 and n are frequency independent factors [23]. The n values varies from 0 to 1, where $n = 1$ represents pure capacitor and $n = 0$ represents pure resistor. The constant phase element (CPE) value for Pure Gellan gum is 30 μF and for various compositions of (0.8, 1.0, 1.1, 1.2 M wt %) NH$_4$SCN salt with 1 g Gellan gum, the CPE values are 141 μF, 237 μF, 131 μF, and 577 μF, respectively. The n value of pure Gellan gum is 0.4998. For 1 g Gellan gum with various compositions of (0.8, 1.0, 1.1, 1.2 M wt %) NH$_4$SCN salt, the n values are 0.7916, 0.6982, 0.7666, and 0.7224, respectively. The conductivity for the various compositions is provided in Table 5 below.

From Table 5, it is noted that the conductivity increases, as the concentration of ammonium thiocyanate is increased; i.e., as we increase the concentration of salt, the charge carrier concentration increases. The conductivity is maximum for 1 g Gellan gum with 1.1 M wt% of NH$_4$SCN, 1.41×10^{-2} S/cm and the Rb, CPE, and n values for 1 g Gellan gum with 1.1 M wt% of NH$_4$SCN are 49, 131, and 0.7666. S. Selvalakshmi et al. has reported that the composition of 50 Agar: 50 NH$_4$SCN gives the conductivity of about 1.03×10^{-3} S/cm [36]. G. Nirmala devi et al. has reported for the composition, 60Dextrin:40NH$_4$SCN providing the conductivity of 4.05×10^{-4} S/cm [41]. M. Muthukrishanan et al. reported for the bio polymer composition 40 Pectin: 60 NH$_4$SCN having the conductivity, 1.5×10^{-3} S/cm [42]. Though M J Neto et al. [66] has reported that Gellan doped with choline-based IL N,N,Ntrimethyl-N-(2-hydroxyethyl)ammonium bis (trifluoromethylsulfonyl) imide ([N$_{1\ 1\ 2(OH)}$][NTf$_2$]) (5:1) exhibits an ionic conductivity of 5.21×10^{-6} S cm^{-1} and 3.83×10^{-5} at 30 °C and 90 °C, there is no much new

Table 4 Electrochemical impedance spectroscopy (EIS) parameters

Compositions	R (Ω)	CPE (μF)	n (no unit)
1 g pure Gellan gum	1646	30	0.4998
1 g Gellan gum + 0.8 M wt% of NH_4SCN	729	141	0.7916
1 g Gellan gum + 1.0 M wt% of NH_4SCN	94	237	0.6982
1 g Gellan gum + 1.1 M wt% of NH_4SCN	*49*	*131*	*0.7666*
1 g Gellan gum + 1.2 M wt% of NH_4SCN	64	577	0.7224

Italic emphasizes R, CPE and n value of the highest conducting polymer electrolyte

researches on ammonium salts with Gellan gum. Polymer membrane, 1 g Gellan gum with 1.1 M wt% of NH_4SCN has got highest ionic conductivity of $1.41 \pm 0.09 \times 10^{-2}$ S/cm. This membrane has got more amorphous nature (XRD) and low glass transition temperature (42.98 °C). For 1 g of Gellan gum with 1.2 M wt% of NH_4SCN, the conductivity decreases. Even though the concentration of the NH_4SCN increases, the charge carriers may also increased. But they form aggregate, which leads to the decrease in conductivity.
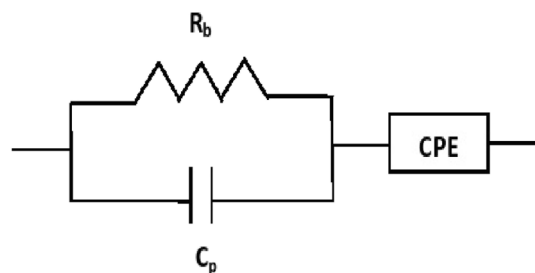
Transference number measurement

Transference number measurement gives information about the nature of the charge carriers. This transference number measurement can be done using the Wagner's polarization technique.

From the Wagner's polarization, we can calculate the transference number of the polymer electrolyte sample corresponding to the ionic (t_{ion}) and electronic (t_-) transport number.

Fig. 7 **a** Cole-cole plot of 1 g pure Gellan gum. **b** Equivalent circuit of pure Gellan gum
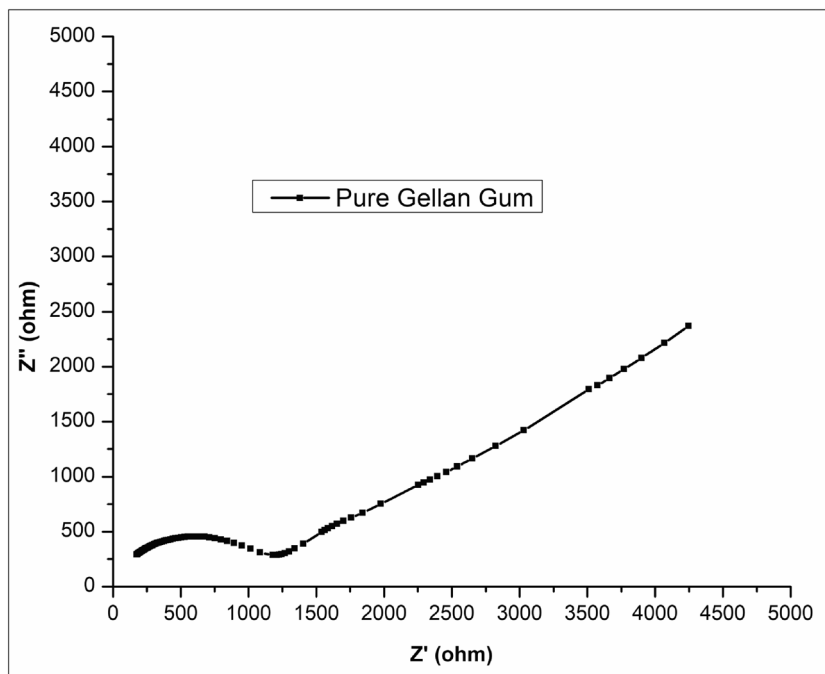
(a)

(b)

Fig. 8 **a** Various concentrations of NH$_4$SCN (0.8 M wt%, 1.0 M wt%, 1.1 M wt%, 1.2 M wt%) with 1 g Gellan gum. **b** Equivalent circuit of highest ionic conducting polymer electrolyte (1.1 M wt% with 1 g Gellan gum)
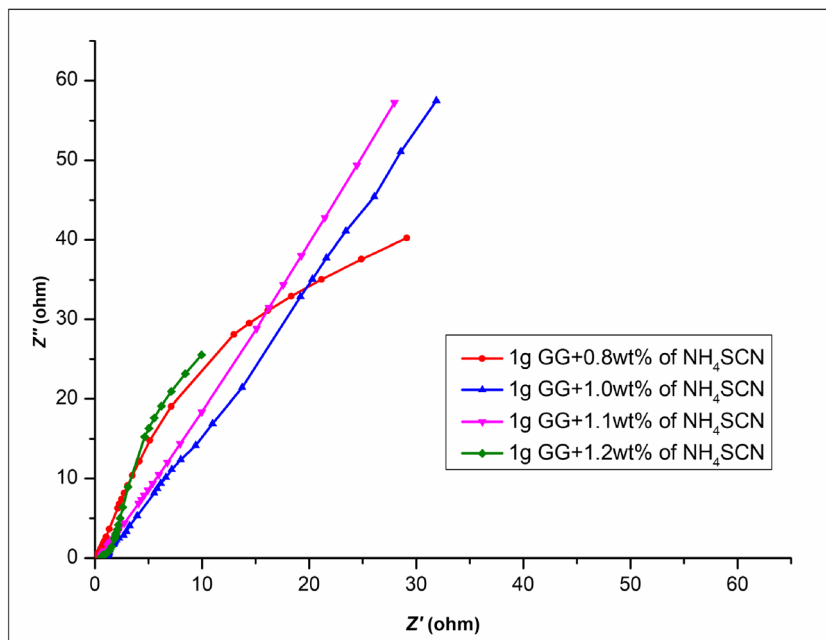
(a)
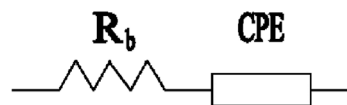
(b)

The high conducting electrolyte sample is placed in between two stainless steel electrodes. The initial current was noted when the DC voltage of 1.5 V is connected to the cell. As the time increases, the current gradually decreases and it becomes stable and the final current is measured.

From the initial and final current noted, the transference number of ion and electron can be measured.

$$t_+ = \frac{I_i - I_f}{I_i}$$

$$t_- = \frac{I_f}{I_i}$$

where

t_+	transference number of cation
t_-	transference number of anion
I_i	initial current
I_f	final current

From the above equation, we could find that the $t_+ = 0.99$; $t_- = 0.01$. This confirms that the conductivity is mainly contributed by the ions [67, 68]. The drop in current and the saturation pattern can be noted in Fig. 9.

Construction of a proton conducting battery

The successfulness of a proton conducting battery depends on the anode (which must be capable of supplying the H$^+$ ions into the electrolyte), the highest ion conducting polymer electrolyte, and the cathode.

Table 5 The conductivity values for various concentrations of NH$_4$SCN salt with Gellan gum

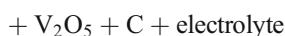| Compositions	Conductivity
1 g pure Gellan gum	$4.22 \pm 0.14 \times 10^{-6}$ S/cm
1 g Gellan gum + 0.8 M wt% of NH$_4$SCN	$9.80 \pm 0.06 \times 10^{-4}$ S/cm
1 g Gellan gum + 1.0 M wt% of NH$_4$SCN	$2.01 \pm 0.03 \times 10^{-3}$ S/cm
1 g Gellan gum + 1.1 M wt% of NH$_4$SCN	*$1.41 \pm 0.09 \times 10^{-2}$ S/cm*
1 g Gellan gum + 1.2 M wt% of NH$_4$SCN	$1.64 \pm 0.12 \times 10^{-3}$ S/cm

Fig. 9 Variation of DC current for time for the composition 1 g Gellan gum: 1.1 M wt % of NH$_4$SCN (high conductivity sample) using Wagner's method
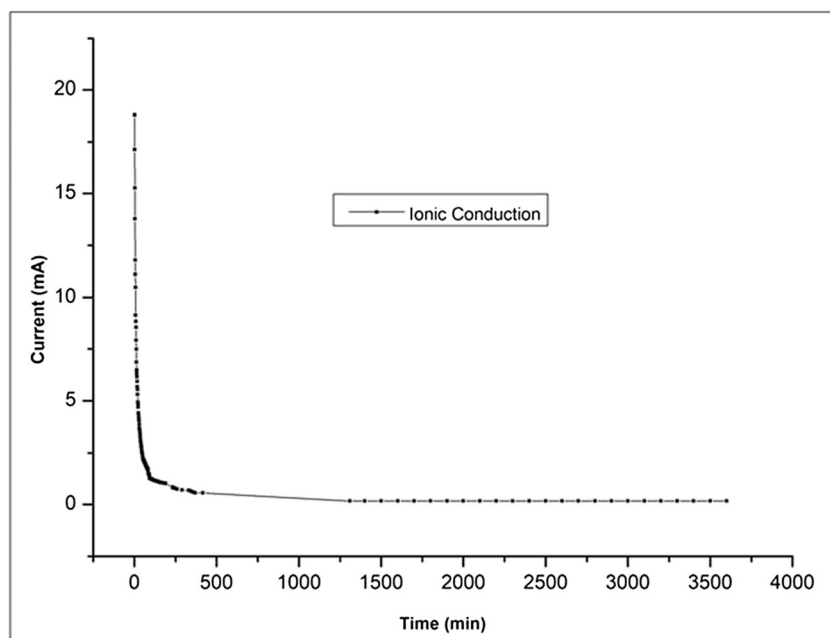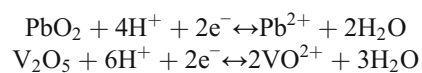

The composition of lead dioxide (4 g), vanadium pentoxide (1 g), and graphite (0.5 g) were grinded well for nearly 2 h, and the highest conducting polymer electrolyte 0.25 g is added to the mixture and grinded well. There are few reports [45, 46, 69] using PbO$_2$ and V$_2$O$_5$ mixture as cathode materials that give best performance.

The anodic material is prepared from the mixture of zinc metal powder (3 g), zinc sulphate (1 g), and graphite (1 g); the mixture was grinded well. Due to the superiority property than the other metals, the metallic zinc is preferred in anode compartment [45, 46, 69].
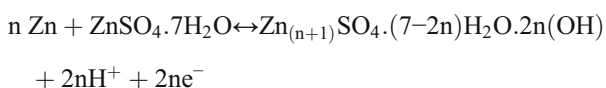
The constructed battery has the following structure.

Zn + ZnSO$_4$.7H$_2$O

+ C||1 g Gellan Gum + 1.1 M wt%of NH$_4$SCN||PbO$_2$

+ V$_2$O$_5$ + C + electrolyte

The cathode reaction is

$$PbO_2 + 4H^+ + 2e^- \leftrightarrow Pb^{2+} + 2H_2O$$
$$V_2O_5 + 6H^+ + 2e^- \leftrightarrow 2VO^{2+} + 3H_2O$$

The anode reaction is

$$n\ Zn + ZnSO_4.7H_2O \leftrightarrow Zn_{(n+1)}SO_4.(7-2n)H_2O.2n(OH)$$

+ 2nH$^+$ + 2ne$^-$

The prepared mixture for cathode and anode are made into pellets using pellatizer by giving pressure of about 5 ton. The anode was placed in the battery holder, over which the highest conducting polymer electrolyte and the cathode were placed. The set up is drawn (Fig. 10).

The cell exhibited the *open circuit voltage of 1.62V*. With the load of 100kΩ, the cell exhibits the OCV of 1.62 V (Fig. 11 a and b) and the current drawn from it is 16 μA, decreased to 1.2V, and the setup was retained for 60 h. The discharge voltage with respect to the time is plotted as graph (Fig. 12). The stabilized voltage retained is called plateau region, after which the voltage of the cell is decreased. The initial decrease in the voltage may be used to the polarization [70]. The cell parameters of the constructed cell are shown in Table 6.
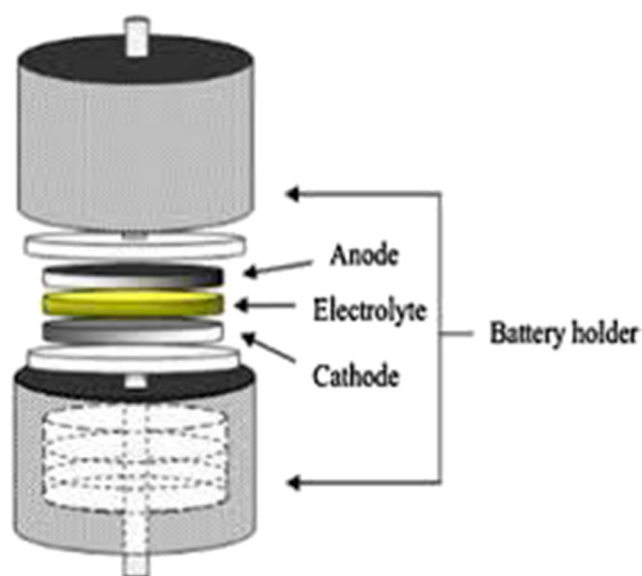

Fig. 10 Setup of a battery

Table 6 Cell parameters

S. no	Cell parameters	1 g Gellan gum + 1.1 M wt % of NH$_4$SCN
1	Open circuit voltage (OCV)	1.62 V
2	Current drawn	16 μA
3	Weight of the cathode	0.490 g
4	Weight of the anode	0.556 g
5	Weight of the electrolyte	0.145 g
6	Weight to the cell	1.191 g
7	Thickness of cathode	1.309 mm
8	Thickness of anode	1.497 mm
9	Area of the cell	1.1304 cm^2
10	Discharge time	60 h
11	Current density	14.154 μA/cm^2

Fig. 11 Open circuit voltage for 1 g Gellan gum: 1.1 M wt % of NH$_4$SCN
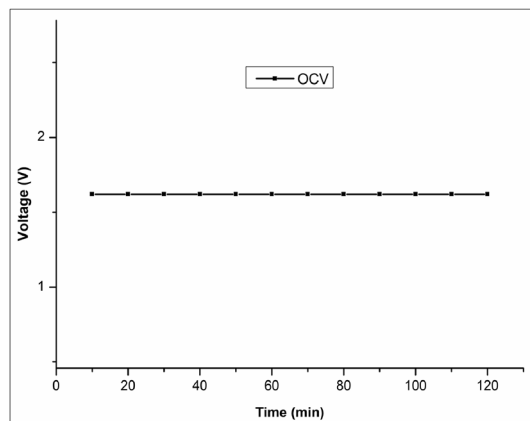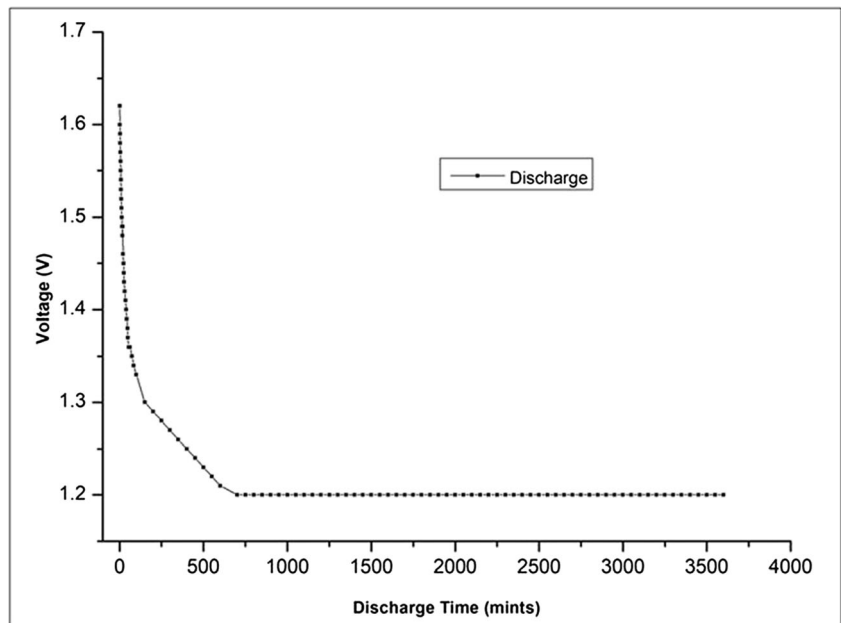

Fig. 12 Discharge curve for the cell having the highest conductivity (1 g Gellan gum: 1.1 M wt % of NH$_4$SCN)
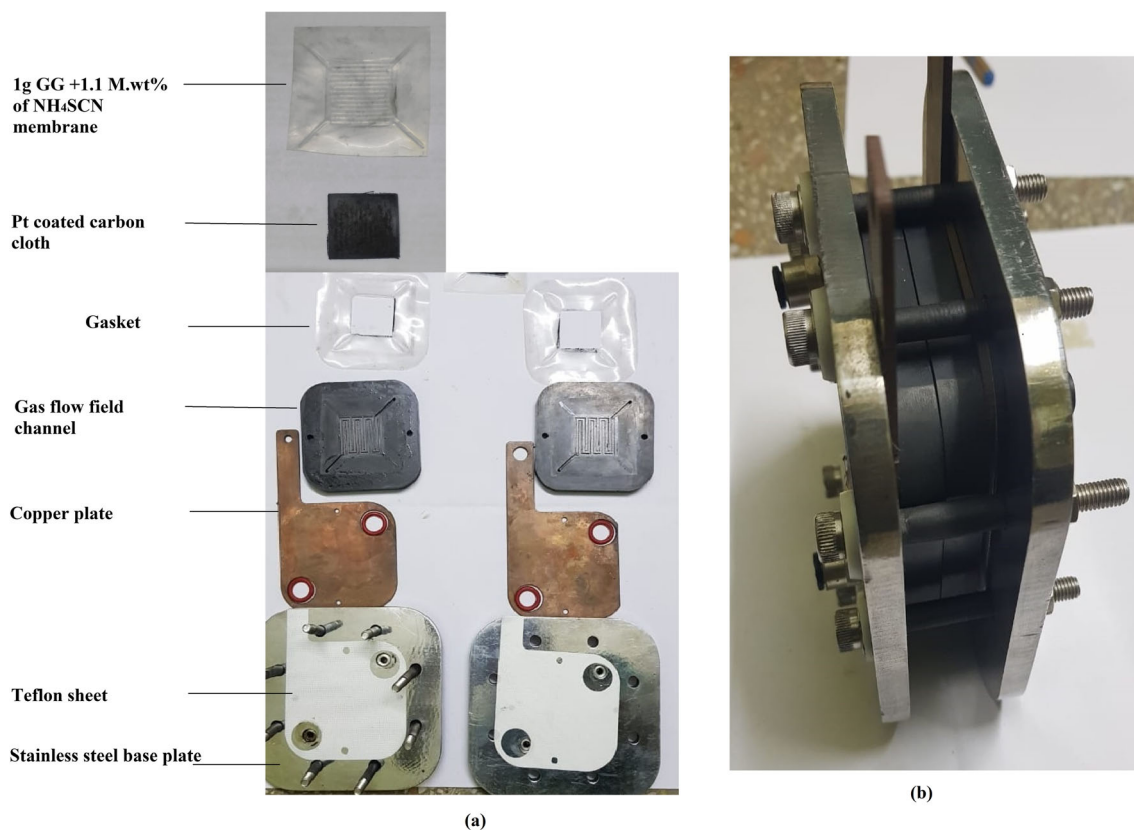
Fig. 13 **a** Parts of fuel cell. **b** Constructed fuel cell

Construction of fuel cell

The proton exchange membrane (PEM) fuel cell is an electro-chemical device that can operate at room temperature. The fuel cell consist of bipolar graphite plates, with the electrodes made up of carbon cloth coated with the platinum over the surface uniformly at the rate of 0.3 mg/cm. This electrode, the platinum coated carbon cloth, acts as the catalyst layer for the chemical reaction.

The base plate of the fuel cell is made of stainless steel over which the Teflon sheet is covered to avoid the contact between the copper plate and the steel. The highest conducting (1 g Gellan gum with 1.1 M wt% of NH_4SCN) sample is sandwiched in between the bipolar graphite plate as described further. The bipolar graphite plate has the parallel flow channel size of 7.84 cm^2.

The platinum coated carbon cloths of area ~8.41 cm^2, which are the electrodes placed on the either sides of the highest conducting membrane and is covered with the gasket of thickness 0.2 mm. This setup is placed over the copper plate and again another set of copper plate over which the Teflon sheet and stainless steel base plate were placed and tightened thoroughly. This is the set up of single PEM fuel cell (Fig. 13).

An electrolyser (Fig. 14) is used to produce hydrogen and oxygen gas. The electrolyser is operated under DC voltage supply of 2V. The 80 ml of oxygen and 100 ml of hydrogen gases per min are passed through the single PEM fuel cell, and the anode and the cathode reactions are given below.
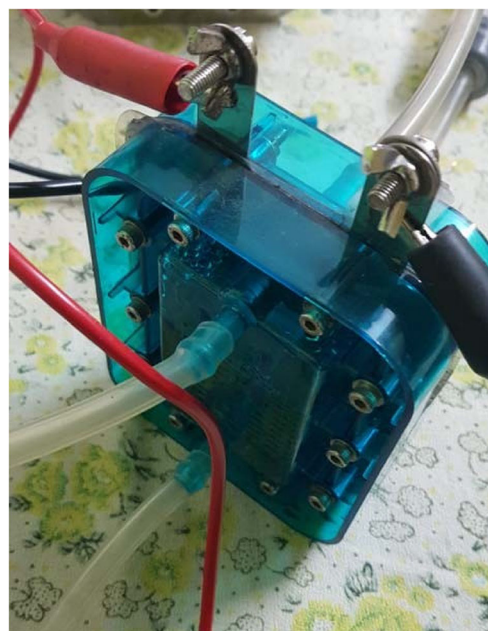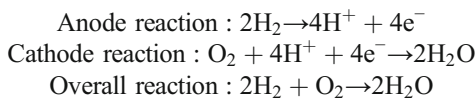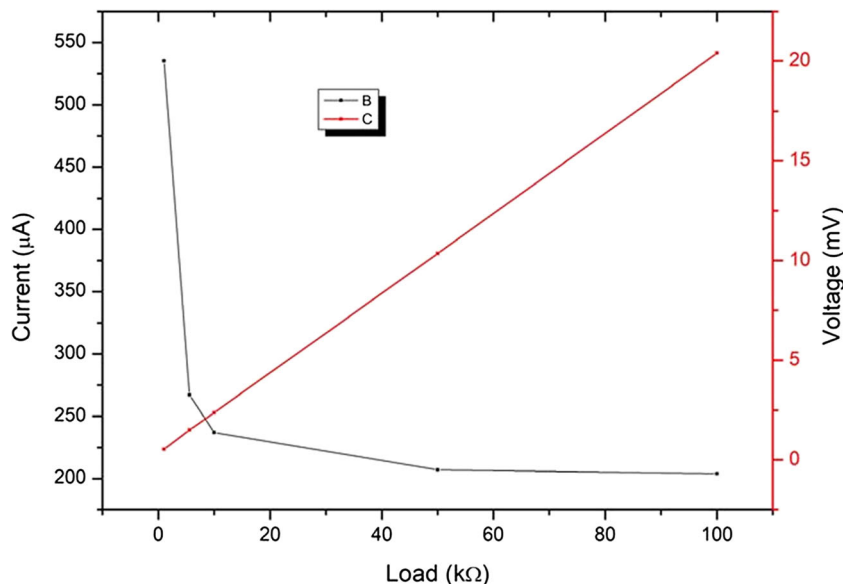

Fig. 14 Electrolyser

Table 7 Current and voltage for various load connected in the fuel cell

Load (kΩ)	Current (μA)	Voltage (mV)
1	535	0.535
5.6	267	1.495
10	237	2.37
50	207	10.35
100	204	20.4

Fig. 15 Variation of current and voltage for various loads (1 kΩ, 5.6 kΩ, 10 kΩ, 50 kΩ, and 100 kΩ) for 1 g Gellan gum with 1.1 M wt% of NH_4SCN

$$\text{Anode reaction}: 2H_2 \rightarrow 4H^+ + 4e^-$$
$$\text{Cathode reaction}: O_2 + 4H^+ + 4e^- \rightarrow 2H_2O$$
$$\text{Overall reaction}: 2H_2 + O_2 \rightarrow 2H_2O$$

Various load such as 1kΩ, 5.6 kΩ, 10 kΩ, 50 kΩ, and 100 kΩ are connected across the fuel cell, and the current and voltage are measured which are given in Table 7 and the graph plotted is represented in Fig. 15.
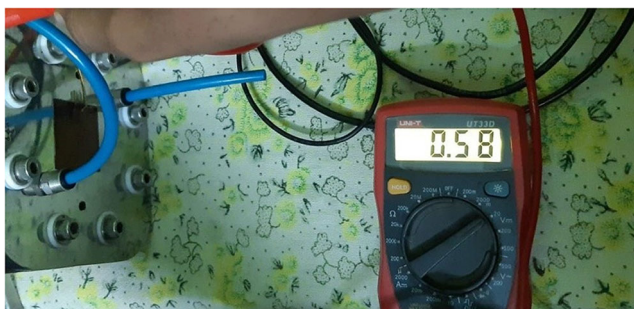

Fig. 16 Open circuit voltage of single PEM fuel cell for 1 g Gellan gum: 1.1 M wt% of NH_4SCN

The fuel cell potential for the highest conducting polymer electrolyte is measured as *580 mV* (Fig. 16). Moniha et al. has reported the fuel cell potential of 442 mV [43] and 503 mV [45] for i-carrageenan with NH_4NO_3 and i-carrageenan with NH_4SCN. G. Boopathi et al. [34] has reported that the fuel cell potential for agar with NH_4NO_3 is found to be 558 mV. S. Selvalakshmi et al [46] reported the output potential of 500 mV.

Conclusion

Using the Solution Casting Technique bio polymer Gellan gum with various compositions of NH_4SCN has been prepared, and the conductivity of the highest conducing membrane is found to be 1.41×10^{-2} S/cm for *1 g Gellan gum + 1.1 M wt% of NH_4SCN*. XRD results confirm the *amorphous nature* of the highest conducting biopolymer, and its crystallinity percentage is *8.85%*. FTIR explains the complex formation between the polymer and salt. Using the highest conducting membrane, 1.1 M wt% of NH_4SCN with 1 g Gellan gum, proton conducting battery, and fuel cell has been fabricated and is found to perform with the cell potential of *1.62 V* and *580 mV*.

References

1. Long L, Wang S, Xiao M, Meng Y (2016) Polymer electrolytes for lithium polymer batteries. J Mater Chem A 4(26):10038–10069

2. Fergus JW (2010) Ceramic and polymeric solid electrolytes for lithium–ion batteries. J Power Sources 195(15):4554–4569

3. Maccullum JR, Vincent CA (eds) (1987) Polymer electrolyte reviews. Elsevier, London

4. Bruce PG, Campbell SA, Lightfoot P, Mehta MA (1995) Polymer electrolytes: structure and electrode processes. Solid State Ionics 78:191–198

5. Blonsky M, Claney S, Hardy LC, Harris CS, Spinder R, Tonge JS, Shriver DF (1989) Polymereic Electrolytes Chem Tech:758

6. Bozkurt A (2002) Application of proton conducting polymer electrolytes to electrochemical devices. Turk J Chem 26:663–668

7. Lewandowski A, Zajder M, Frackowiak E, Begim F (2001) Supercapacitors based on activated carbon and poly(ethylene oxide)-KOH-H2O polymer electrolyte. Electrochim Acta 46:2777–2780

8. Chen N, Hong L (2002) Proton conducting membrane composed of sulfonated polystyrene microspheres, poly(vinylpyrrolidone) and poly(vinylidene fluoride). Solid State Ionics 146:377–385

9. Klassem B et al (1998) Raman spectra and transport properties of lithium perchlorate in ethylene carbonate based binary solvent systems for lithium batteries. J Phys Chem B 102(2):4795–4801

10. Shriver DF, Bruce PG (1995) In: Bruce PG (ed) Solid-state electrochemisty. Cambridge, Cambridge University, Press

11. Song JY, Wang YY, Wan CC (1999) Review of gel-type polymer electrolytes for lithium-ion batteries. J Power Sources 77:181–197

12. Qiao J, Hamaya T, Okada T (2005) New highly proton-conducting membrane poly(vinylpyrrolidone) (PVP) modified poly(vinyl alcohol)/2-acrylamido-2-methyl-1-propanesulfonic acid (PVA–PAMPS) for low temperature direct methanol fuel cells (DMFCs). Polymer 46:10809–10816

13. Wieczurek W, Florjanczyk Z, Zukowska G, Borkowska R, Kuzma P, ZygadloMonikowska E, Kuzwa K (2002) Ambient and subambient temperature proton-conducting polymer gel electrolytes. Solid State Ionics 154-155:45–49

14. Subba Reddy CV, Sharmanad AK, Narasimha Rao VVR (2004) Characterization of a solid state battery based on polyblend of (PVP+PVA+KBrO3) electrolyte. Ionics 10:142–147

15. Meng C, Liu C, Chen L, Hu C, Fan S (2010) Highly flexible and all-solid-state aer like polymer super capacitors. Nano Lett 10:4025–4403

16. Fang J, Qiao J, Wilknson DP, Zhang J (eds) (2015) Electrochemical polymer electrolyte membranes. CRC Press, New York

17. Lu D, Xio C, Xu S (2009) Starch-based completely biodegradable polymer materials. Express Polym Lett 3:366–375

18. Ponez L, Sentanin F, Maid S, Arof A, Pawlicka A (2012) Ion conducting membranes based on gelating and containing LiI/I2 for electrochromic devies. Mol Cryst Liq Cryst 554:239–251

19. Ramesh S, Arof AK (2001) Ionic conductivity studies of plasticized poly(vinyl chloride) polymer electrolytes. Mater Sci Eng B 85:11–15

20. Selva Kumar K, Ramesh Prabhu M Int J ChemTech Res 201(6):5740

21. Sikkanthar S, Karthikeyan S, Selvasekarapandian S, Vinoth Pandi D, Nithya S, Sanjeeviraja C (2015) Electrical conductivity characterization of polyacrylonitrile-ammonium bromide polymer electrolyte system. J Solid State Electrochem 19:987–999

22. Sikkanthar S, Karthikeyan S, Selvasekarapandian S, Arunkumar D, NIthya H, Junichi K (2016) Structural, electrical conductivity and transport analysis of PAN-NH4Cl polymer electrolyte system. Ionics 22:1085–1094

23. Karthikeyan S, Sikkanthar S, Selvasekarapanidan S, Arunkumar D, Nithya H, Kawamura J (2016) Structural, electrical and electrochemical properties of polyacrylonitrile-ammonium hexaflurophosphate polymer electrolyte system. J Polym Res 23:51

24. Sivadevi S, Selvasekarapandian S, Karthikeyan S, Sanjeeviraja C, Nithya H, Iwa Y, Kawamura J (2015) Proton-conducting polymer electrolyte based on PVA-PAN blend doed with ammonim thiocyanate. Ionics 21:1017–1029

25. Vijaya N, Selvasekarapandian S, Hirankumar G, Karthikeyan S, NIthiya H, Ramya CS, Praabu M (2012) Structural, vibrational, thermal, and conductivity studies on proton-conducting polymer electrolyte based on poly (N-vinylpyrrolidone). Ionics 18:91–99

26. Ramalingaiah S, Srinivas Reddy D, Jaipal Reddy M, Laxminarsaiah E, Subba Rao UV (1996) Conductivity and discharge characteristic studies of novel polymer electrolyte based on PEO complexed with Mg(NO3)2 salt. Mater Lett 29:285–289

27. Nechifor CD, Ciobanu CL, Dorohoi DO, Ciobanu C (2009) UPB Sci. Bull Series A 71:97–106

28. Hemalatha R, Alagar M, Selvasekarapandian S, Sundaresan B, Moniha V, Boopathi G, Christopher Selvin P (2019) Preparation and characterization of proton-conducting polymer electrolyte based on PVA, amino acid proline, and NH4Cl and its applications to electrochemical devices. Ionics 25:141–154

29. Hemalatha R, Alagar M, Selvasekarapandian S, Suaresan B, Moniha V (2019) Studies of proton conducting polymer electrolyte based on PVA, amino acid proline and NH4SCN. J Sci: Adv Mater Devices 4(1):101–110

30. Vinoth Pandi D, Selvasekarapandian S, Bhuvaneswari R, Premalatha M, Monisha S, Arunkumar D, Junichi K (2016) Development and characterization of proton conducting polymer electrolyte based on PVA, amino acid glycine and NH4SCN. Solid State Ionics 298:15–22

31. Subramaniyan SELVASEKAPANDIAN, Muthusamy HEMA, Junichi KAWAMURA, Osamu KAMISHIMA, Rangaswami BASKARAN (2010) Characterization of PVA-NH4NO3 polymer electrolyte and its application in rechargeable proton battery. J Phys Soc Jpn 79:163–168

32. Nusrath Unnisa C, Chitra S, Selvasekarapandian S, Monisha S, Nirmala Devi G, Moniha V, Hema M (2018) Development of poly(glycerol suberate) polyester (PGS)-PVA blend polymer electrolytes with NH4SCN and its appolications. Ionics 24:1979–1993

33. Rajendran S, Uma T (2000) Characterization of plasticized PMMA–LiBF4 based solid polymer electrolytes. Bull Mater Sci 23:27–29

34. Boopathi G, Pugalendhi S, Selvasekarapandian S, Premalatha M, Monisha S, Aristatil G (2017) Development of proton conducting biopolymer membrane based on agar-agar for fuel cell. Ionics 23:2781–2790

35. Selvalakshmi, T. Mathavan, S. Selvasekarapandian, M. Premalatha. A study on Agar – Agar – NH4I biopolymer electrolytes. DAE Solid State Physics Symposium (2017). AIP Conference Proc. 1942, 140019-1 - 140019-4

36. Selvalakshmi, N. Vijaya, S. Selvasekarapandian, M. Premalatha. (2017) Biopolymer agar-agar doped with NH4SCN as solid polymer electrolyte for electrochemical cell application. J Appl Polym Sci 134 (15):44702. https://doi.org/10.1002/app.44702

37. Monisha S, Selvasekarapandian S, Mathavan T, Milton Franklin Benial A, Manoharan S, Karthikeyan S (2016) Preparation and characterization of biopolymer electrolyte based on cellulose acetate for potential applications in energy storage devices. J Mater Sci Mater Electron 27:9314–9324

38. Monisha S, Mathavan T, Selvasekarapandian S, Benial AMF, Aristatil G, Mani N, Premalatha M, Vinoth Pandi D (2017) Investigation of biopolymer electrolyte based on cellulose acetate-ammonium nitrate for potential use in electrochemical devices. Carbohydr Polym 157:38–47

39. Premalatha M, Mathavan T, Selvasekarapandian S, Monisha S, Vinoth Pandi D, Selvalakshmi S (2016) Investigations on proton conducting biopolymer membranes based on tamarind seed polysaccharide incorporated with ammonium thiocyanate. J Non-Cryst Solids 453:131–140

40. Premalatha M, Mathavan T, Selvasekarapandian S, Selvalakshmi S, Monisha S (2017) Incorporation of NH4Br in Tamarind Seed Polysaccharide Biopolymer and its potential use in electrochemical energy storage devices. Organ Electon 50:418–425

41. Nirmala Devi G, Citra S, Selvasekarapandian S, Premalatha M, Monisha S (2017) Synthesis and characterization of dextrin-based biopolymer electrolytes for potential applications in energy storage devices. Ionics 23:3377–3388

42. Muthukrishnan M, Shanthi C, Selvasekarapandian S, Manjladevi R, Perumal P, Chrishtopher Selvin P (2019) Synthesis and characterization of pectin-based biopolymer electrolyte for electrochemical applications. Ionics 25:203–214

43. Moniha V, Alagar M, Selvasekarapandian S, Sundaresan B, Boopathi G (2018) Conductive biopolymer electrolyte iota-carrageenan with ammonium nitrate for application in electrochemical devices. J Non-Cryst Solids 481:424–434

44. Karthikeyan S, Selvasekarapandian S, Premalatha M, Monisha S, Boopathi G, Aristatil G, Arun A, Madeswaran S (2017) Proton-conducting I-Carrageenan-based biopolymer electrolyte for fuel cell application. Ionics 23:2775–2780

45. Moniha V, Alagar M, Selvasekarapandian S, Sundaresan B, Hemalatha R, Boopathi G (2018) Synthesis and characterization of bio-polymer electrolyte base on iota-carrageenan with ammonium thiocyanate and its applications. J Solid State Electrochem 22(10):1–15

46. Selvalakshmi S, Mathavan T, Selvasekarapadian S, Premalatha M (2019) Characterization of biodegradable solid polymer electrolye system based on agar-NH4Br and its comparison with NH4I. J Solid State Electochem 23:1727–1737

47. Ramaiah S, Kumar TMP, Ravi V (2007) Studies on biopolymers for ophthalmic drug. J Macromolec Sci A 44:229

48. Jansson PE, Lindberg B, Sandford A (1983) Structural studies of gellan gum, an extracellular polysaccharide elaborated by Pseudomonas elodea. Carbohydr Res 124:135–139

49. Giavasis I, Harvey LM, McNeil B (2000) Gellan cum. Crit Rev Biotechnol 20:177–211

50. Milas M, Shi X, Rinaudo M (1990) On the physicochemical properties of gellan gum. Biopolymers 30:451–464

51. Shah J (2007) Gellan Gum and its Applications-A Review.

52. Majid SR, Sabadini RC, Kanicki J, Pawlicka A (2014) Impedance analysis of gellan gum-poly(vinyl pyrrolidone) membranes. Mol Cryst Liq Cryst 604(1):84–95

53. Noor ISM, Majid SR, Arof AK, Djurado D, Claro Neto S, Pawlicka A (2012) Characteristics of gellan gum-LiCF$_3$SO$_3$ polymer electrolytes. Solid State Ionics 225:649–653

54. Noor IM (2020) Determination of charge carrier transport properties of gellan gum-lithium triflate solid polymer electrolyte from vibrational spectroscopy. High Perfrom Polym 32(2):168–174

55. Chandra S, Hashmi SA, Prasad G (1990) Studies on ammonium perchlorate doped polyethylene oxide polymer electrolyte. Solid State Ionics 40-41:651–654

56. Kumar M, Sekhon S (2002) Role of Plasticizer's dielectric constant on conductivity modification of PEO-NH4F polymer electrolytes Eur. Oly. 38:1297–1304

57. Gray FM (1991) Solid Polymer Electrolytes. VCH Publishers Inc, New York

58. Hodge RM, Edward GH, Simon GP (1996) Water absorption and states of water in semicrystalline poly(vinyl alcohol) films. Polymer 37:1371–1376

59. Karthika JS, Vishalakshi B, Naik J (2016) Gellan gum–graft–polyaniline—an electric conducting biopolymer. Int J Biol Macromol 82:61–67

60. Singh R, Bhattacharya B, Rhee H-W, Singh PK (2015) Solid Gellan gum polymer electrolyte for energy application. Int J Hydrog Energy 40:9365–9372

61. Sudhamania SR, Prasada MS, Sankar KU (2003) DSC and FTIR studies on Gellan and polyvinyl alcohol (PVA) blend films. Food Hydrocoll 17:245–250

62. Halim NFA, Majid SR, Arof AK, Kajzar F, Pawlicka A (2012) Gellan Gum- LiI Gel Polymer Electrolytes. Mol Cryst Liq Cryst 554(1):232–238

63. Abarna S, Hirankumar G (2017) Electrical, dielectric and electrochemical studies on new li ion conducting solid polymer electrolytes based on polyethylene glycol p-tert-octylphrnyl ether. Funct Polym 59:660–668

64. Macdonald JR (ed) (1987) Impedance Spectroscopy. John Wiley & Sons, New York, pp 12–23

65. Boukamp BA (1986) Solid State Ionics 20:301

66. Neto MJ, Sentanin F, Espernca JMSS, Medeiros MJ, Pawlicka A, de Zea Bermudez V, Silva MM (2015) Gellan gum-ionic liquid membranes for electrochromic device application. Solid State Ionics 274:64–70

67. Woo HJ, Majid SR, Arof AK (2011) Transference number and structural analysis of proton conducting polymer electrolyte based on poly (ε-caprolactone). Mater Res Innov 15(s2):s49–s54

68. Shukur MF, Kadir MFZ (2015) Electrical and transport properties of NH4Br-doped cornstarch based solid biopolymer electrolyte. Ionics 21(1):111–112

69. Maheshwari T, Tamilarasan K, Selvasekarapandian S, Chitra R, Kiruthika S (2021) Investigation of blend biopolymer electrolytes based on Dextran-PVA with ammonium thiocyanate. J Solid State Electrochem 25(3):755–765

70. Subba Reddy CV, Sharma AD, Narasimha Rao VVR (2003) Conductivity and discharge characteristics of polyblend (PVP+PVA+KIO3) electrolyte. J Power Sources 114:338–345